

## Appendix 1 Flow in an annular channel

The cylindrical symmetry of an annular channel suggests the use of cylindrical polar coordinates, as illustrated in Figure A 1.1 below. Consider an annular element of fluid at radius  $r$ , of thickness  $\delta r$  and length  $\delta x$ . The area of the end cross-section of the element is  $2\pi r\delta r$  and the area,  $A$ , of the cylindrical surface of the element is  $2\pi r\delta x$ . The element moves with steady velocity  $u$  in the positive  $x$ -direction and is in equilibrium with a pressure difference across its ends due to a pressure gradient,  $dP/dx$ , and shear force,  $\tau$ , on its sides.

The channel is also an annulus, with inner radius  $r_i$  and outer radius  $r_o$ .

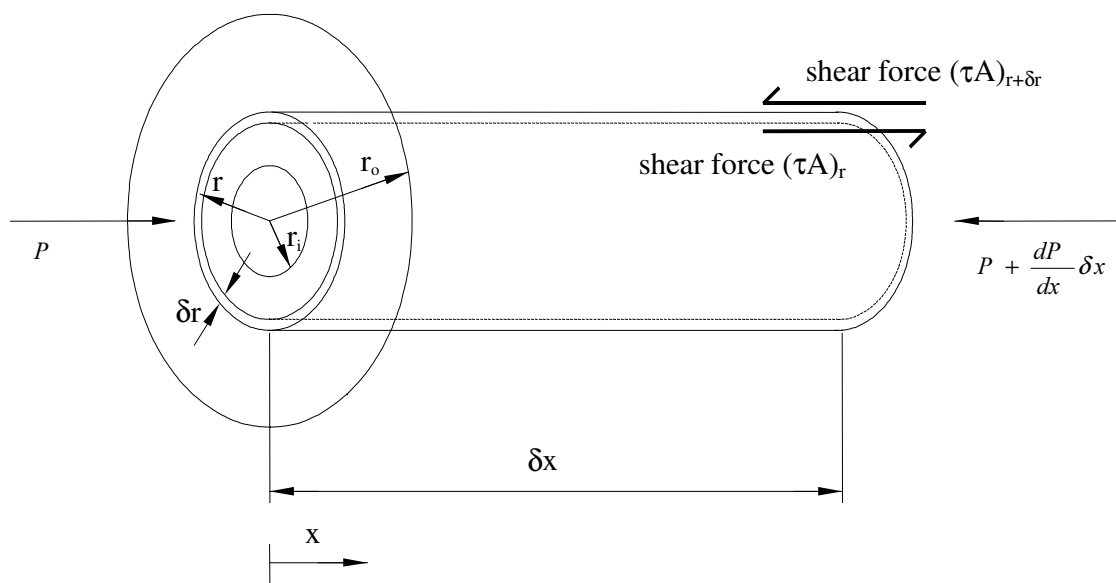


Figure A 1.1 Fluid element and coordinate system for flow in an annular channel

### A1.1 Equation of motion

In steady flow the element has no acceleration and its equation of motion reduces to an expression of equilibrium:

$$\left\{ P - \left( P + \frac{dP}{dx} \delta x \right) \right\} 2\pi r \delta r + (\tau A)_r - (\tau A)_{r+\delta r} = 0. \quad (\text{A } 1.1)$$

If the thickness of the element is small the variation of shear force with radius can be assumed to be linear, reducing the equation of motion to:

$$-\frac{dP}{dx} \delta x 2\pi r \delta r - \frac{\partial}{\partial r} (\tau A) \delta r = 0. \quad (\text{A } 1.2)$$

In a Newtonian fluid such as water, the shear stress is given by  $\tau = \mu \partial u / \partial r$ . Using this and the earlier expression for the area  $A$  of the surface of the element,

$$\frac{\partial}{\partial r} \left( \mu r \frac{\partial u}{\partial r} \right) = -r \frac{dP}{dx}. \quad (\text{A } 1.3)$$

This expression is simply Poisson's equation for  $u$  in cylindrical polar coordinates with rotational and axial symmetry. A more general formulation of the equation of motion for the non-symmetrical case, where shear stress is allowed to vary as a function of angle as well as radius, yields:

$$\nabla^2 u = \frac{1}{r} \frac{\partial}{\partial r} \left( r \frac{\partial u}{\partial r} \right) + \frac{1}{r^2} \frac{\partial^2 u}{\partial \theta^2} + \frac{\partial^2 u}{\partial x^2} = -\frac{1}{\mu} \frac{dP}{dx}. \quad (\text{A } 1.4)$$

Returning to the original, simpler, expression and integrating twice with respect to  $r$ , assuming that  $dP/dx$  is a function only of  $x$ , yields an expression for velocity:

$$u = -\frac{r^2}{4\mu} \frac{dP}{dx} + B \ln r + C. \quad (\text{A } 1.5)$$

The constants of integration  $B$  and  $C$  can be found on substitution of two appropriate boundary conditions.

## A1.2 Annular channel, two solid boundaries

If both boundaries of the channel are solid surfaces, the axial velocity must be zero at each wall, in this case at radii  $r = r_i$  and  $r = r_o$ . This yields a relationship between velocity and pressure gradient as a function of radius:

$$u = \frac{1}{4\mu} \frac{dP}{dx} \left\{ r_i^2 - r^2 + \frac{(r_o^2 - r_i^2)}{\ln(r_o/r_i)} \ln(r/r_i) \right\}. \quad (\text{A 1.6})$$

The volumetric flow rate,  $Q$ , can be calculated by integrating the velocity expression over the cross-section of the channel:

$$\begin{aligned} Q &= \int_{r_i}^{r_o} 2\pi r u \, dr \\ &= \frac{\pi}{2\mu} \frac{dP}{dx} \int_{r_i}^{r_o} r_i^2 r - r^3 + \frac{(r_o^2 - r_i^2)}{\ln(r_o/r_i)} r \ln(r/r_i) \, dr \\ &= \frac{\pi}{2\mu} \frac{dP}{dx} \left[ \frac{r_i^2 r^2}{2} - \frac{r^4}{4} + \frac{(r_o^2 - r_i^2)}{\ln(r_o/r_i)} \frac{r^2}{2} (\ln r - 1/2) - \frac{(r_o^2 - r_i^2)}{\ln(r_o/r_i)} \frac{r^2}{2} \ln r_i \right]_{r_i}^{r_o} \\ &= \frac{\pi}{8\mu} \frac{dP}{dx} \left\{ r_o^4 - r_i^4 - \frac{(r_o^2 - r_i^2)^2}{\ln(r_o/r_i)} \right\}. \end{aligned} \quad (\text{A 1.7})$$

Wall shear stress can be determined by evaluating  $\mu \partial u / \partial r$  at the appropriate radius:

$$\tau = \mu \frac{\partial u}{\partial r} = - \left( \frac{r}{2} + \frac{r_o^2 - r_i^2}{4r \ln(r_o/r_i)} \right) \frac{dP}{dx}. \quad (\text{A 1.8})$$

Substituting  $r = r_o$  to find the shear at the outside wall of the channel,

$$\tau_w = - \left( \frac{2r_o^2 \ln(r_o/r_i) - r_o^2 + r_i^2}{4b \ln(r_o/r_i)} \right) \frac{dP}{dx}, \quad (\text{A 1.9})$$

or shear can be equivalently expressed as a function of flow rate using the earlier relationship between flow rate and pressure drop as:

$$\tau_w = - \frac{2\mu}{\pi r_o} \frac{r_i^2 - r_o^2 (1 - 2 \ln(r_o/r_i))}{(r_o^4 - r_i^4) \ln(r_o/r_i) - (r_o^2 - r_i^2)^2} Q. \quad (\text{A 1.10})$$

### A1.3 Annular channel, one solid boundary, one free surface

If now only one boundary of the channel is a solid surface, the axial velocity at that boundary must be zero, in this case at a radius  $r = r_o$ . If the other boundary is a free surface, shear there must be zero, equivalently  $\partial u / \partial r = 0$ , here at radius and  $r = r_i$ . Substitution of these two conditions in the same way as above yields the following relationship between velocity and pressure gradient as a function of radius:

$$u = \frac{1}{4\mu} \frac{dP}{dx} \left\{ r_o^2 - r^2 + 2r_i^2 \ln(r/r_o) \right\}. \quad (\text{A 1.11})$$

The volumetric flow rate,  $Q$ , can again be calculated by integrating the velocity expression over the cross-section of the channel:

$$\begin{aligned} Q &= \int_{r_i}^{r_o} 2\pi r u \, dr \\ &= \frac{\pi}{8\mu} \frac{dP}{dx} \left\{ r_o^4 - 4r_i^2 r_o^2 + r_i^4 (3 + 4 \ln(r_o/r_i)) \right\}. \end{aligned} \quad (\text{A 1.12})$$

Wall shear stress can be determined by evaluating  $\mu \partial u / \partial r$  at the appropriate radius:

$$\tau = \mu \frac{\partial u}{\partial r} = - \left( \frac{r}{2} - \frac{r_i^2}{2r} \right) \frac{dP}{dx}. \quad (\text{A 1.13})$$

Substituting  $r = r_o$  to find the shear at the outside wall of the channel,

$$\tau_w = - \frac{1}{2r_o} (r_o^2 - r_i^2) \frac{dP}{dx}, \quad (\text{A 1.14})$$

or shear can be equivalently expressed as a function of flow rate using the earlier relationship between flow rate and pressure drop as:

$$\tau_w = - \frac{4\mu}{\pi r_o} \frac{r_o^2 - r_i^2}{r_o^4 - 4r_i^2 r_o^2 + r_i^4 (3 + 4 \ln(r_o/r_i))} Q. \quad (\text{A 1.15})$$

## Appendix 2 Flow in a semicircular pipe

### A2.1 Velocity distribution

The boundary conditions for a semicircular pipe suggest the use of a polar coordinate system, as illustrated in Figure A 2.1 below:

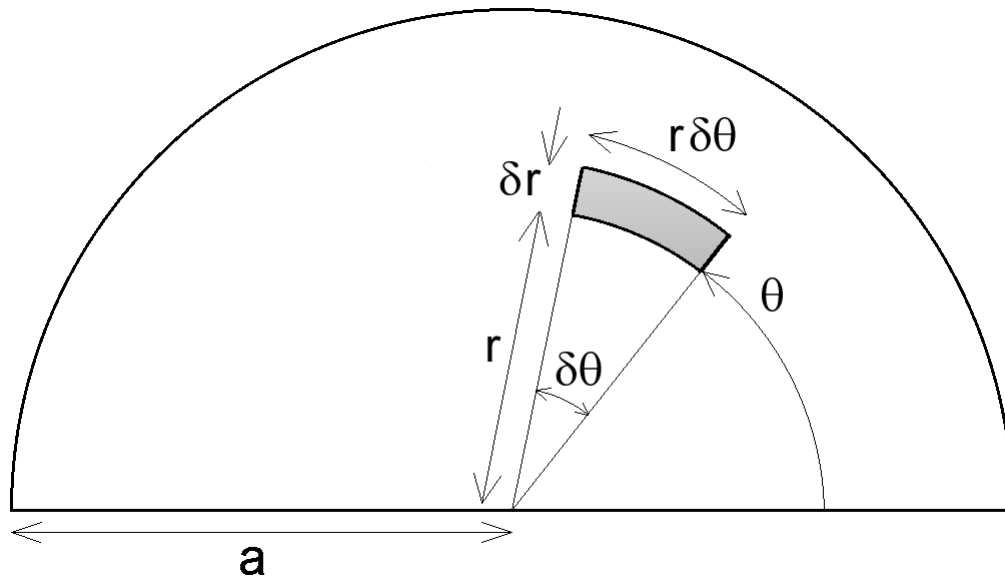


Figure A 2.1 Polar coordinate system for semicircular pipe

Equation (A 1.4) above gives the general form of the equilibrium equation for an element of a viscous fluid subject to a pressure gradient. The boundary conditions for a semicircular pipe are simplified if the radial coordinate,  $r$ , is non-dimensionalised by the substitution  $r' = r/a$ , where  $a$  is the radius of the pipe:

$$\frac{\partial^2 u}{\partial r'^2} + \frac{1}{r'} \frac{\partial u}{\partial r'} + \frac{1}{r'^2} \frac{\partial^2 u}{\partial \theta^2} = -\frac{a^2}{\mu} \frac{dP}{dx}. \quad (\text{A 2.1})$$

A solution is sought to Equation (A 2.1), which is consistent with the boundary condition for a semicircular pipe that  $u = 0$  when  $\theta = 0$  and  $\pi$ . Expansion of the right-hand side of the equation using a Fourier sine series yields:

$$\frac{\partial^2 u}{\partial r'^2} + \frac{1}{r'} \frac{\partial u}{\partial r'} + \frac{1}{r'^2} \frac{\partial^2 u}{\partial \theta^2} = -\frac{a^2}{\mu} \frac{dP}{dx} \sum_{n=1,3,5,\dots}^{\infty} \frac{4}{n\pi} \sin n\theta, \quad (\text{A } 2.2)$$

which suggests a sinusoidal solution, of the form:

$$u = \sum_{n=1,3,5,\dots}^{\infty} f_n(r') \sin n\theta. \quad (\text{A } 2.3)$$

Substituting the trial solution into Equation (A 2.2) gives the following equation:

$$\sum_{n=1,3,5,\dots}^{\infty} \left( \frac{\partial^2 f}{\partial r'^2} + \frac{1}{r'} \frac{\partial f}{\partial r'} - \frac{n^2 f}{r'^2} \right) \sin n\theta = -\frac{4a^2}{\mu\pi} \frac{dP}{dx} \sum_{n=1,3,5,\dots}^{\infty} \frac{1}{n} \sin n\theta. \quad (\text{A } 2.4)$$

For complete generality this relationship must be satisfied for arbitrary  $n$  and  $\theta$ , that is,

$$\frac{\partial^2 f}{\partial r'^2} + \frac{1}{r'} \frac{\partial f}{\partial r'} - \frac{n^2 f}{r'^2} = -\frac{4a^2}{\mu\pi n} \frac{dP}{dx}. \quad (\text{A } 2.5)$$

This ordinary differential equation is easily solved for  $f$  using the complementary function/particular integral method, with the boundary condition that  $u = 0$  when  $r' = 1$ .  $f$  is therefore given by:

$$f = \frac{4a^2}{\mu\pi} \frac{dP}{dx} \left( \frac{r'^n}{n(2-n)(2+n)} - \frac{r'^2}{n(2-n)(2+n)} \right), \quad (\text{A } 2.6)$$

and the general expression for the velocity distribution across the pipe cross-section which results is:

$$u = \frac{4a^2}{\mu\pi} \frac{dP}{dx} \left( \sum_{n=1,3,5,\dots}^{\infty} \frac{r'^n \sin n\theta}{n(2-n)(2+n)} - r'^2 \sum_{n=1,3,5,\dots}^{\infty} \frac{\sin n\theta}{n(2-n)(2+n)} \right). \quad (\text{A } 2.7)$$

The variation of velocity,  $u$ , with radius and angle is illustrated in Figure A 2.2 below. As required by the boundary conditions,  $u$  is zero at the walls of the pipe and a maximum near

the centre. By differentiating the velocity expression, Equation (A 2.7), the maximum velocity is found to occur at a radius  $r' = 0.480$ .

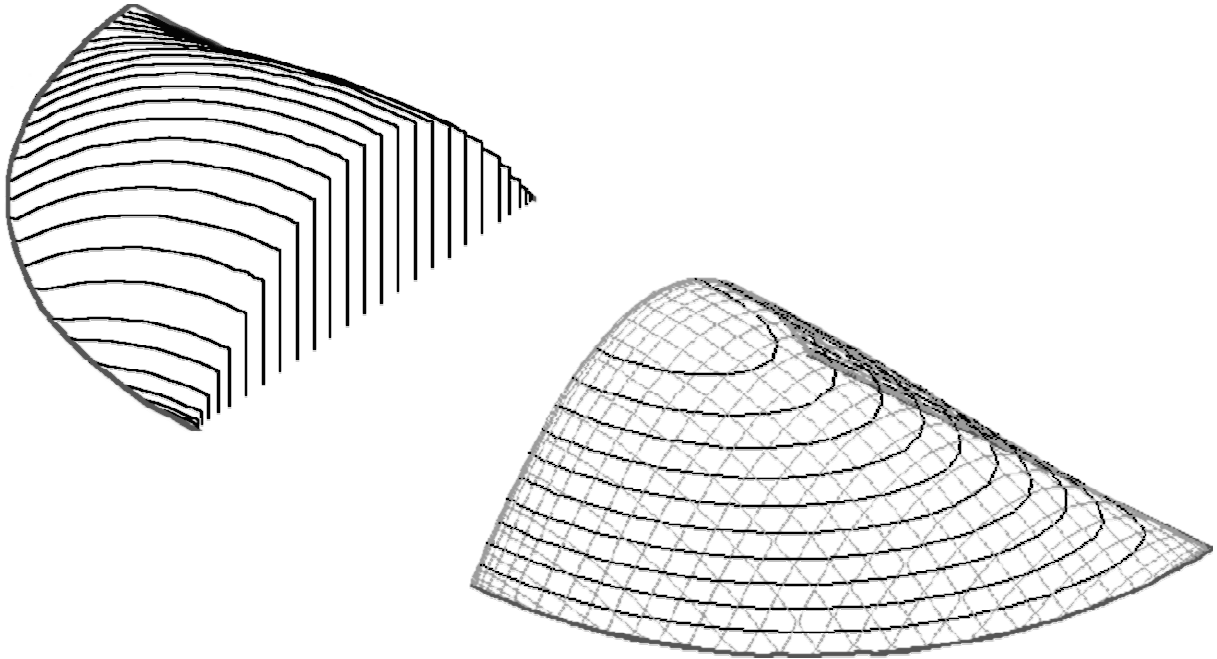


Figure A 2.2 Velocity distribution in semicircular pipe

### A2.2 Volumetric flow rate

The flow rate through the pipe can now be determined by integration of the velocity across the pipe section:

$$Q = \int u \, dA = a^2 \int_{\theta=0}^{\pi} \int_{r'=0}^1 u r' \, dr' \, d\theta. \quad (\text{A 2.8})$$

Substituting for velocity from Equation (A 2.7) above,

$$Q = \frac{4a^4}{\mu\pi} \frac{dP}{dx} \sum_{n=1,3,5,\dots}^{\infty} \left( \int_{\theta=0}^{\pi} \int_{r'=0}^1 \left\{ \frac{r'^{n+1} \sin n\theta}{n(2-n)(2+n)} - \frac{r'^2 \sin n\theta}{n(2-n)(2+n)} \right\} dr' \, d\theta \right). \quad (\text{A 2.9})$$

Firstly the integration with respect to  $r'$  is performed:

$$Q = \frac{4a^4}{\mu\pi} \frac{dP}{dx} \sum_{n=1,3,5,\dots}^{\infty} \left( \int_{\theta=0}^{\pi} \left\{ \frac{\sin n\theta}{n(2-n)(2+n)^2} - \frac{\sin n\theta}{4n(2-n)(2+n)} \right\} d\theta \right). \quad (\text{A 2.10})$$

Secondly the integration with respect to  $\theta$  is carried out, yielding:

$$Q = \frac{4a^4}{\mu\pi} \frac{dP}{dx} \sum_{n=1,3,5,\dots}^{\infty} \left( \frac{2}{n^2(2-n)(2+n)^2} - \frac{1}{2n^2(2-n)(2+n)} \right). \quad (\text{A 2.11})$$

The use of partial fractions allows considerable simplification of the above, to:

$$Q = \frac{a^4}{2\mu\pi} \frac{dP}{dx} \sum_{n=1,3,5,\dots}^{\infty} \left( \frac{1}{n^2} + \frac{1}{(2+n)^2} - \frac{1}{n} + \frac{1}{(2+n)} \right). \quad (\text{A 2.12})$$

The  $1/n^2$  and  $1/(2+n)^2$  terms, and the  $1/n$  and  $1/(2+n)$  terms respectively are very nearly the identical, since each pair of terms represent the same element shifted by one term in the series summation. Further simplification is therefore possible, to:

$$Q = \frac{a^4}{2\mu\pi} \frac{dP}{dx} \left( \left\{ \sum_{n=1,3,5,\dots}^{\infty} \frac{2}{n^2} \right\} - 2 \right), \quad (\text{A 2.13})$$

and hence finally,

$$Q = \frac{a^4}{2\mu\pi} \frac{dP}{dx} \left( \frac{\pi^2}{4} - 2 \right). \quad (\text{A 2.14})$$

### A2.3 Wall shear stress

A correction is necessary to express shear stress along the flat face of the semicircular pipe in terms of the polar coordinates employed. At a given value of radial coordinate,  $\rho$ , wall shear stress is given by:

$$\tau = \frac{\mu}{\rho a} \frac{\partial u}{\partial \theta}. \quad (\text{A 2.15})$$

Equation (A 2.7) above may therefore be differentiated and substituted into Equation (A 2.15) to yield:

$$\tau = \frac{4a}{\pi} \frac{dP}{dx} \left( \sum_{n=1,3,5,\dots}^{\infty} \frac{r'^{n-1} \cos n\theta}{(2-n)(2+n)} - r' \sum_{n=1,3,5,\dots}^{\infty} \frac{\cos n\theta}{(2-n)(2+n)} \right). \quad (\text{A } 2.16)$$

By symmetry, only half of the pipe wall need be considered. This expression is therefore simplified as when  $\theta = 0$ ,  $\cos n\theta = 1$ . The average shear stress may be obtained by integrating the local shear stress over the half of the wall for which  $\theta = 0$ :

$$\begin{aligned} \bar{\tau} &= \int_0^1 \tau(r') dr' \\ &= \frac{4a}{\pi} \frac{dP}{dx} \left[ \sum_{n=1,3,5,\dots}^{\infty} \frac{r'^n}{n(2-n)(2+n)} - \sum_{n=1,3,5,\dots}^{\infty} \frac{r'^2}{n(2-n)(2+n)} \right]_0^1 \\ &= \frac{4a}{\pi} \frac{dP}{dx} \left( \sum_{n=1,3,5,\dots}^{\infty} \frac{1}{2n(2+n)} \right). \end{aligned} \quad (\text{A } 2.17)$$

The use of partial fractions yields the simple result that:

$$\bar{\tau} = \frac{a}{\pi} \frac{dP}{dx}, \quad (\text{A } 2.18)$$

or using Equation (A 2.14) to express mean wall shear stress in terms of flow rate,  $Q$ ,

$$\bar{\tau} = \frac{8\mu}{(\pi^2 - 8)a^3} Q. \quad (\text{A } 2.19)$$

The same method may be used to evaluate the mean shear stress on the curved wall of the pipe as:

$$\bar{\tau} = \frac{4\mu(\pi^2 - 4)}{\pi(\pi^2 - 8)a^3} Q. \quad (\text{A } 2.20)$$

Mean shear stress on the straight wall of a semicircular pipe is therefore higher than on the curved wall, but only by about 7%.

### Appendix 3 Numerical simulation of the Thomas adsorption model

Assuming that adsorption rate is characterised by Langmuir-type kinetics, it may be simply predicted using Equation ( 5.1 ) introduced above. Continuity of the protein solution yields an expression for the rate of change of mobile-phase concentration, Equation ( 5.23 ). Both equations can be combined into a single partial differential equation that is suitable for solving numerically, to yield a prediction for the time-variation of the concentration at outlet of an affinity separator. The numerical model is more general when expressed in dimensionless form, so the following non-dimensional groups were therefore employed:

Liquid-phase concentration	$C' = C/C_0$
Solid-phase concentration	$q' = q/q_m$
Dimensionless length	$x' = x/L$
Dimensionless time	$t' = ut/L$
Peclet number	$Pe = uL/D$
Membrane loading factor	$\Psi = (1 - \varepsilon)q_m / \varepsilon C_0$
Forward rate factor	$\Theta = k_1 LC_0 / u$
Reverse rate factor	$\Omega = k_1 LK_d / u$

Table A 3.1 Non-dimensional groups for Thomas model simulation

The following central-difference expressions for derivatives were obtained from Taylor series. In the notation, superscript  $n$  refers to the discrete time coordinate, and subscript  $m$  to increments in the spatial coordinate.

$$\frac{\partial C'}{\partial x'} = \frac{C'_{m+1} - C'_{m-1}}{2 \Delta x'}, \quad (\text{A 3.1})$$

$$\frac{\partial C'}{\partial t'} = \frac{C'^{n+1}_m - C'^{n-1}_m}{2 \Delta t'}, \quad (\text{A 3.2})$$

$$\frac{\partial q'}{\partial t'} = \frac{q'^{n+1}_m - q'^{n-1}_m}{2 \Delta t'} \text{ and} \quad (\text{A 3.3})$$

$$\frac{\partial^2 C'}{\partial x'^2} = \frac{C'_{m+1} - 2C'_m + C'_{m-1}}{\Delta x'^2} = \frac{C'_{m+1} - C'_m - C'_m + C'_{m-1} + C'_m}{\Delta x'^2}. \quad (\text{A 3.4})$$

The non-dimensional version of the solid-phase concentration equation ( 5.1 ) was:

$$\frac{\partial q'}{\partial t'} = \Theta C'(1 - q') - \Omega q'. \quad (\text{A 3.5})$$

The finite-difference version of the differential was inserted into this expression, which was then rearranged to make  $q'^{n+1}_m$  the subject. The method of Hwu<sup>56</sup> was applied, in which  $q'^n_m$

was approximated by  $\frac{q'^{n+1}_m + q'^{n-1}_m}{2}$  to ensure convergence of the solution, with a similar

substitution for  $C'^n_m$ . The resulting expression was thus:

$$q'^{n+1}_m = \frac{q'^{n-1}_m + 2 \Delta t' \left[ \frac{\Theta}{2} (C'_{m-1} + C'_{m+1}) \left( 1 - \frac{q'^{n-1}_m}{2} \right) - \frac{\Omega}{2} q'^{n-1}_m \right]}{1 + 2 \Delta t' \left[ \frac{\Theta}{4} (C'_{m-1} + C'_{m+1}) + \frac{\Omega}{2} \right]}. \quad (\text{A 3.6})$$

A similar procedure was applied to the material balance, Equation ( 5.23 ), to yield an expression for the liquid-phase concentration:

$$C'^{n+1}_m = \frac{C'^{n-1}_m + 2 \Delta t' \left[ \frac{(C'_{m+1} - C'_m + C'_{m-1})}{Pe \Delta x'^2} - \frac{(C'_{m+1} - C'_{m-1})}{2 \Delta x'} - \frac{\Psi}{2 \Delta t'} (q'^{n+1}_m - q'^{n-1}_m) \right]}{1 + \frac{2 \Delta t'}{Pe \Delta x'^2}}. \quad (\text{A 3.7})$$

The initial conditions were straightforward—at the start of each experiment there was no BSA present in the membrane, either in solution or adsorbed to the solid phase. Mathematically,  $C' = q' = 0$  for all  $x$ , when  $t' = 0$ .

The boundary conditions of Dankwerts<sup>34</sup> were used. These allow for axial diffusion at the inlet side of the membrane, and mixing at the outlet side. Mathematically, these are:

$$\varepsilon u C - \varepsilon D \frac{\partial C}{\partial x} = \varepsilon u C_0 \text{ at } x = 0, t \geq 0, \text{ and} \quad (\text{A } 3.8)$$

$$\frac{\partial C}{\partial x} = 0 \text{ at } x = L, t \geq 0. \quad (\text{A } 3.9)$$

The non-dimensional versions of these conditions are respectively:

$$C' - \frac{1}{Pe} \frac{\partial C'}{\partial x'} = 1 \text{ at } x' = 0, t' \geq 0, \text{ and} \quad (\text{A } 3.10)$$

$$\frac{\partial C'}{\partial x'} = 0 \text{ at } x' = 1, t' \geq 0. \quad (\text{A } 3.11)$$

Initial conditions were applied and the solid-phase concentration for the first time increment calculated using Equation (A 3.6) above at successive space increments, from the inlet to the outlet side of the membrane. Once the solid-phase concentration was known at all spatial positions, the liquid-phase concentration could then be evaluated at the same time-step by Equation (A 3.7). The process was thus essentially the same as that described by Najarian<sup>85</sup>, but for this study the Matlab software package was used to run the simulation rather than a Fortran program. Being matrix-based, the Matlab environment is a convenient platform for solving a two-dimensional differential equation, with many tools for processing and visualisation of the simulation output.

Below is a sample of the Matlab file used to calculate and display the breakthrough curves in Section 5.9.3 for BSA with an Immobilon-CD ion-exchange membrane, using the above

finite-difference equations. When a comparison with the experimental breakthrough curve was necessary, as in Figure 5.21, the non-dimensional time axis of the model was converted to dimensional time by a scaling factor determined by integration of the experimental breakthrough curve.

The continuous stirred-tank reactor model of Suen and Etzel<sup>104</sup> was also incorporated. The governing equation for the CSTR is simply:

$$V_D \frac{dC_{out}}{dt} = Q(C_{in} - C_{out}), \quad (\text{A } 3.12)$$

where  $C_{in}$  is the concentration of the solution entering the CSTR, of volume  $V_D$ , and  $C_{out}$  the concentration at the CSTR exit. This equation was cast into a form suitable for application to the numerical simulation using a forward difference expression.

### A3.1 Matlab breakthrough program listing

```

Q=0.98;
C0=0.928;
N=2;

dia=2.3;
t=0.0112;
porosity=0.7;
Vdead=6.1;
qm=51;
Kd=0.0693;
k1=0.0421;
Pe=0.1;

A=pi*dia^2/4;
L=t*N;
velocity=Q/A/porosity;
psi=(1-porosity)/porosity*qm/C0;
theta=k1*L*C0/velocity;
omega=k1*Kd*L/velocity;

```

---

```

nx=51;
dx=1/(nx-1);
nt=15000;
dt=0.002;
C=zeros(nt,nx);
q=zeros(nt,nx);
c=zeros(nt,1);

    for n=3:nt
        for m=2:(nx-1)
            q(n,m)=(q(n-2,m)+2*dt*(theta/2* ...
(C(n-1,m-1)+C(n-1,m+1))*(1-q(n-2,m)/2)- ...
omega/2*q(n-2,m)))/(1+2*dt*(theta/4*(C(n-1,m-1)+ ...
C(n-1,m+1))+omega/2));
            C(n,m)=(C(n-2,m)+2*dt* ...
(- (C(n-1,m+1)-C(n-1,m-1))/2/dx+ ...
(C(n-1,m+1)-C(n-2,m)+C(n-1,m-1))/Pe/dx^2- ...
psi/2/dt*(q(n,m)-q(n-2,m)))/(1+2*dt/Pe/dx^2);
        end
%boundary conditions:
        C(n,1)=(Pe*dx+C(n,2))/(1+Pe*dx);
        q(n,1)=(q(n-2,1)+2*dt* ...
(theta*C(n-1,1)*(1-q(n-2,1)/2)-omega/2*q(n-2,1)))/ ...
(1+2*dt*(theta/2*C(n-1,1)+omega/2));
        C(n,nx)=C(n,(nx-1));
        q(n,nx)=(q(n-2,nx)+2*dt* ...
(theta*C(n-1,nx)*(1-q(n-2,nx)/2)-omega/2*q(n-2,nx)))/ ...
(1+2*dt*(theta/2*C(n-1,nx)+omega/2));
        c(n)=(c(n-2)+2*dt*Q/Vdead*(C(n-1,nx)-c(n-2)/2))/ ...
(1+Q*dt/Vdead);
    end

T=(linspace(0,dt*(nt-1),nt))';
hold on
plot(T,C(:,nx),'b-')
plot(T,c,'r:')
grid on;
axis([-1 3 0 1])

wklwrite('Tvec',T)
wklwrite('outlet',C(:,nx))
wklwrite('cstr',c)

```

## Appendix 4 Approximate analytical solutions for adsorption

The following sections introduce the approximate solutions for breakthrough when each of the four mechanisms described in Section 5.9 is the sole rate-limiting mechanism. These solutions are plotted in Figure 5.24.

### A4.1 Binding Kinetics

Although solved rigorously with the numerical model detailed in Appendix 3, an approximate solution exists for breakthrough when Langmuir reaction kinetics are rate-limiting. For the case of irreversible equilibrium, Bohart and Adams<sup>17</sup> derived the following solution as long ago as 1920:

$$\frac{C/C_0}{1-C/C_0} = \exp((1-r^*)N_r(T-1)). \quad (\text{A } 4.1)$$

### A4.2 Film Transport

Michaels<sup>77</sup> derived a solution for irreversible equilibria that are limited solely by film diffusion in 1952, as:

$$\frac{C}{C_0} = \exp(N_f(T-1) - 1). \quad (\text{A } 4.2)$$

### A4.3 Pore Diffusion

Vermeulen *et al.*<sup>113</sup> described the course of breakthrough when a pore diffusion mechanism is limiting, again for irreversible equilibria:

$$\frac{C}{C_0} = 1 - \left( \frac{2}{3} - \frac{N_p(T-1)}{3.66} \right)^2. \quad (\text{A } 4.3)$$

#### A4.4 Surface Diffusion

Hall *et al.*<sup>45</sup> derived a solution for the course of breakthrough when solid diffusion was the rate-limiting mechanism, under conditions approaching irreversible binding ( $r^* \approx 0$ ). The simple premise was that the rate of accumulation of diffusing species within a spherical particle was proportional to the difference between the concentration at the surface of the sphere and the average concentration over the whole sphere. This first-order differential equation has the simple differential solution, once boundary conditions are applied, of:

$$\frac{C}{C_0} = 1 - \exp(-\chi_{s,l} N_s (T-1) - 1). \quad (\text{A } 4.4)$$

The term  $\chi_{s,l}$  is a correction factor to match the midpoint slope of the approximation with an exact solution, that depends on the value of the equilibrium parameter  $r^*$ :

$$\chi_{s,l} = \frac{1}{r^{1.06} + 1.125(1-r)^{1.06}}. \quad (\text{A } 4.5)$$